



Calibration of the L3 BGO Calorimeter Using an RFQ Accelerator

A. Favara^a, U. Chaturvedi^a, M. Gataullin^a, G. Gratta^b, D. Kirkby^b, W. Lu^c, H. Newman^a,
A. Shvorob^a, C. Tully^d, R. Zhu^a

^aPhysics Department, California Institute of Technology, Pasadena, CA 91125

^bNow at Stanford University, Stanford, CA 94305

^cNow at Jet Propulsion Laboratory, Pasadena, CA 91109

^dPhysics Department, Princeton University, Princeton, NJ 08544

An improved calibration technique based on a radio-frequency-quadrupole (RFQ) accelerator is presented. A high-intensity flux of 17.6 MeV photons, produced by radiative capture of 1.85 MeV protons from the RFQ in a lithium target, is used to calibrate 11000 crystals of the L3 BGO calorimeter. In this paper, we present results obtained for the calibration of 1997 and 1998 L3 data samples. For the first time a calibration precision better than 0.5% is reached for the entire BGO calorimeter.

1. Introduction

L3 is one of the four experiments operating at the LEP e^+e^- collider at CERN. The L3 electromagnetic calorimeter (ECAL), composed of Bismuth Germanate (BGO) crystals, is one of the key parts of the detector. Crystal detectors are the preferred solution when efficient identification as well as precise energy measurement for electrons and photons are required. BGO crystals of the L3 calorimeter are arranged in two endcaps (each of 1527 crystals) and two half-barrels (7680 crystals combined) [1]. A precision calibration for each crystal is essential to reach the design energy resolution of 1% over the energy range from a few GeV up to 100 GeV.

Prior to the startup of LEP in 1987–88 the barrel of the BGO calorimeter was calibrated using electron beams ranging from 180 MeV to 50 GeV in energy. With approximately 1000 electrons per crystal the achieved precision on the calibration constants was 0.5% [2]. To preserve the energy resolution a precise calibration *in situ* is essential. It is needed to follow the change in response with time of each channel, which is due to changes in the crystal itself or in the electronics chain. In L3, the calibration *in situ* was also essential when the BGO endcaps were installed, in 1991, without any previous test-beam calibration.

Three different calibration techniques have been applied in L3. In the past, there were no sub-1% accuracies: the calibration with cosmic

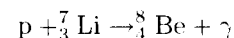
rays reached a precision of 3% [3], and the calibrations based on the Xenon lamps [4] or on the RFQ [5] guaranteed a precision of 1.3%.

In this paper, we present new results for the RFQ calibration which represent a major step forward both in the improved precision and in the reduced systematic effects.

2. RFQ Calibration

2.1. RFQ calibration concept

The RFQ calibration technique uses a pulsed H^- beam from the RFQ accelerator to bombard a lithium target installed inside the BGO calorimeter. After focusing and steering, the beam is neutralised to allow it to pass undisturbed through the magnetic field of L3. Radiative capture of protons



produces 17.6 MeV photons that are used to calibrate the calorimeter.

Figure 1 shows the RFQ system together with the L3 detector. Figure 2 shows the target location inside the BGO calorimeter and the propagation of the calibration photon flux. The RFQ accelerator is synchronised to the ECAL time mark, such that the calibration signal from the photon flux is in time with the integration gate of the ECAL readout. The photon energy spectrum of each crystal is recorded in a readout memory. A veto on the energy deposition in the eight adjacent crystals is implemented to ensure that the

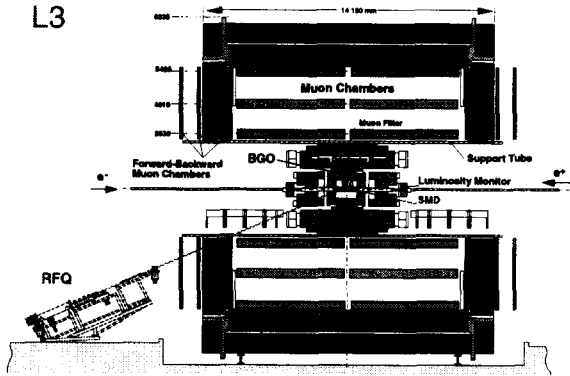


Figure 1. A side view of the L3 detector and the RFQ system.

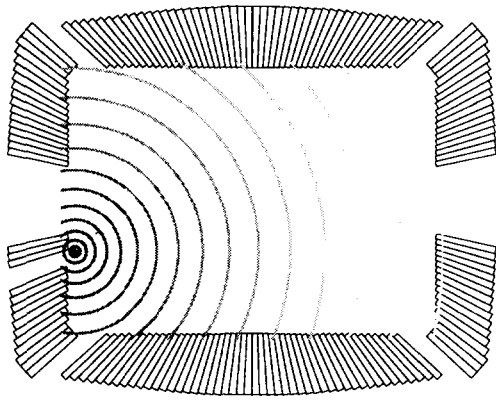


Figure 2. A side view of the BGO calorimeter with concentric circles representing the photon flux originating from the RFQ target.

electromagnetic shower is well contained in a single crystal.

2.2. L3 RFQ calibration system

The L3 RFQ calibration system, shown in Figure 3, was developed by Caltech in collaboration with the World Laboratory. It consists of the following components: a 30 keV RF-driven (2 MHz) volume H^- ion source and a low-energy beam transport; a 1.85 MeV RFQ (425 MHz) accelerator, which can provide an H^- current of 7.5 mA; a high-energy beam transport, consisting of quads and an xy -steering magnet; and a beam neutraliser ($H^- \rightarrow H^0 + e^-$), consisting of a 1 m long N_2 gas cell, at a typical pressure of $5 \cdot 10^{-4}$ Torr corresponding to a neutralisation efficiency of 55%.

The beam enters the L3 detector through a 10 m long beam pipe and reaches a water-cooled

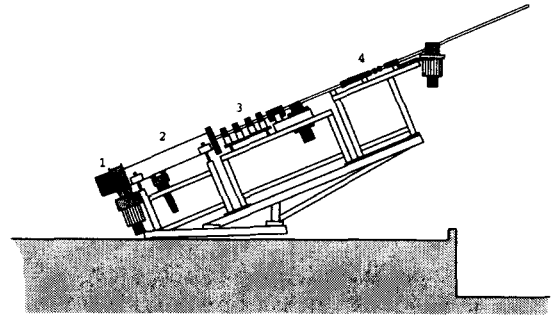


Figure 3. The RFQ system: 1. ion source; 2. RFQ ion accelerator; 3. steering and focusing magnets and 4. beam neutraliser.

LiH target, mechanically sealed with a thin Ta foil, mounted at the end of the beam pipe. More details about the components of the RFQ system can be found in Ref. [6]. Figure 1 shows that the RFQ system is close to the L3 magnet door. A careful shielding from the residual fringe magnetic field was necessary to make the system operational.

2.3. RFQ runs in 1997–98

The last RFQ runs, taken in November 1997 and April 1998, were very successful. The average data acquisition rate was 70 Hz allowing the collection of about 9 million triggers in a few days run.

The quality of the calibration depends on the photon rate; which is characterised by the crystal occupancy, defined as the fraction of triggers with an energy deposition in that crystal larger than 14 MeV. The occupancy differs from crystal to crystal due to the varying location of the crystals relative to the lithium target. The average occupancies were 0.14% and 0.03% in the half-detector on the near and far side, respectively. The occupancy in the half-detector on the far side is shown in Figure 4.

A typical photon energy spectrum deposited in a BGO crystal is shown in Figure 5. For each crystal the calibration constant is given by

$$\text{Cal. Const. (keV/ADC count)} = \frac{E_{HH^+}}{HH^+ - \text{Pedestal}}$$

where the calibration point HH^+ ($E_{HH^+} \approx 17.6$ MeV) is half-way below and to the right of the calibration signal peak. The sharpness of this falling edge ensures that the HH^+ point is the

least sensitive to a variety of possible systematic effects such as the noise level, the incident photon angle and the amount of material in front of the crystal [6]. The values of the calibration constants determined this way are shown in Figure 6 for the near side of the BGO calorimeter. The average value for the calibration constant is 85 keV/ADC channel.

3. Calibration with Bhabha Electrons

At LEP the beam energy is known very precisely* and electrons produced in Bhabha scattering may be used for calibration purposes. Radiative Bhabha events, where the electron energy differs substantially from the beam energy, are efficiently rejected by requiring the electron and positron directions to be opposite.

Using the calibration constants determined with the RFQ run, we obtain an energy resolution for Bhabha electrons of approximately 3%, and we observe shifts in the average energy between 3% and 9%. The main limitation to this calibration method comes from the uncertainty on E_{HH^+} . It is difficult to determine this value very precisely, because it is related to the incident photon angle and the amount of material in front of the crystal. In addition, the extrapolation from the 17 MeV scale to the 100 GeV scale may suffer from non-linearities of the crystal light yield as well as of the electronics chain.

Electrons from Bhabha scattering can also be used to improve the calibration, but this procedure is very delicate and requires a careful analysis. Unfortunately the electromagnetic shower from a high-energy electron is not contained in a single crystal but in a 3×3 crystal matrix (bump) centred on the crystal with the maximum energy deposition. Therefore an inter-calibration, provided by the RFQ system, is needed to start the calibration procedure. In addition, whenever one of the crystals in the bump is noisy or inactive the calibration of all the others will be affected. The same consideration applies for bumps close to the BGO detector's edges, where part of the electromagnetic shower may be lost.

Another drawback is the limited statistics available in the barrel. In 1998, corresponding

*Better than 0.1% and 0.01% at high energy and at the Z peak, respectively.

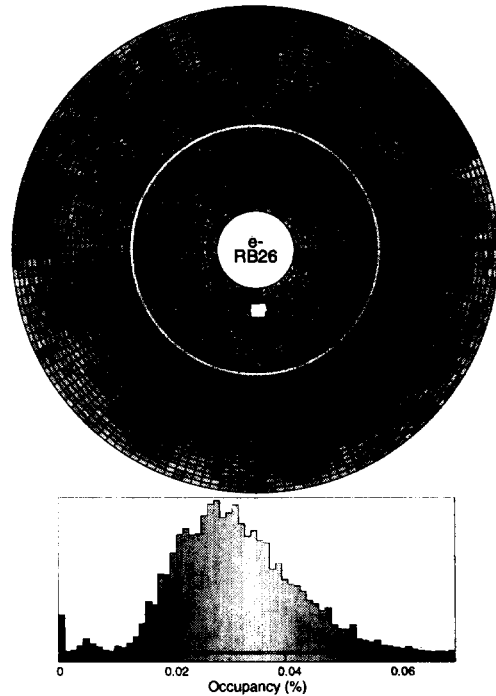


Figure 4. Crystal occupancy for the far half-barrel (outer rings) and endcap (inner rings). The central hole is for the passage of the LEP beam pipe. The smaller hole is for the RFQ beam pipe and target insertion.

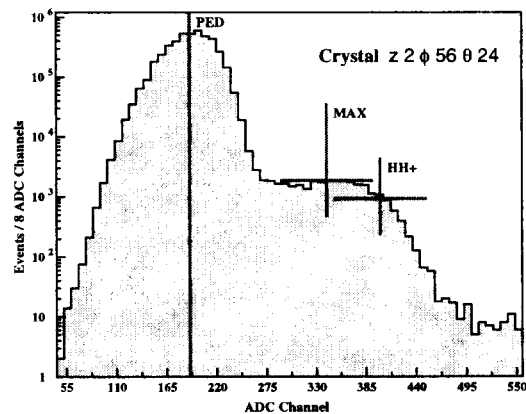


Figure 5. A typical photon energy spectrum shown with the definition of the HH^+ calibration point.

to the highest integrated luminosity ever reached by LEP (about 180/pb per experiment), less than one electron per crystal was available for the calibration of the barrel. As a consequence, old data taken at the Z peak, where the cross section for

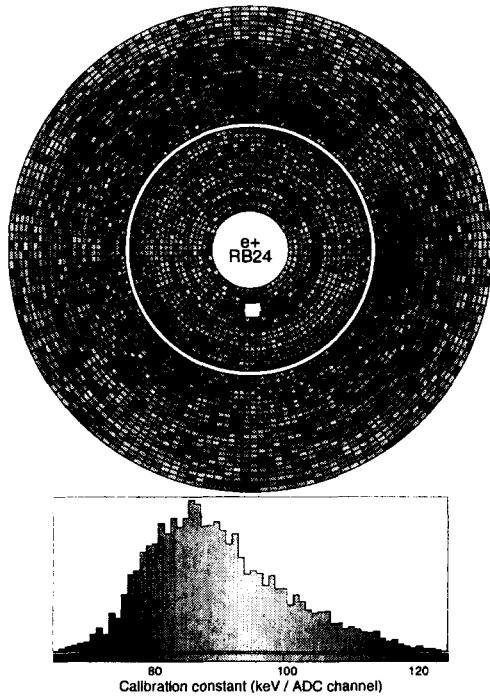


Figure 6. RFQ calibration constants for the near half-barrel (outer rings) and endcap (inner rings).

electrons in the barrel is much higher, should be used as well. But this is not straightforward and several systematic effects, described in the next section, should be taken into account.

Correction factors to the calibration constants obtained with the RFQ system are calculated as follows:

$$\text{Corr. fact.}_j = \frac{1}{\sum_{i=1}^{N_c} w_{ij}} \sum_{i=1}^{N_c} \frac{E_{Beam}}{E_i} w_{ij},$$

where N_c is the number of bumps containing crystal j , E_i is the energy of bump i according to the RFQ calibration, w_{ij} is a weight assigned to bump i proportional to the fractional energy in crystal j , and E_{Beam} is the beam energy. For bumps containing noisy or inactive crystals (about 10% of the total) or laying close to the BGO detector's edges (about 6% of the total) E_i and w_{ij} are obtained by using a shower-fitting algorithm, which provides an estimate of the true energy of the bump and of its exact position.

This procedure is reiterated several times until the correction factors converge to stable values. An independent data sample is used to test

the energy resolution for Bhabha electrons, which reaches the 1% level with the improved calibration.

3.1. Study of systematic effects

When using electrons from Bhabha scattering collected in previous years runs, we should take into account time dependent effects. A decrease of the light yield with time has been observed since the beginning of L3 operation and it is well described by a $1/t$ function. Different slopes are observed for the different parts of the BGO detector, but on average the light yield has decreased by more than 10% over nine years. The evolution of the light yield over the last three years is shown in Figure 7. Different behaviours of the four sub-detectors are observed because they were manufactured and installed in different periods. For instance the endcaps, which show a more pronounced decay, are two years younger. The L3 ECAL aging is most probably due to a degradation of the reflective paint coating the BGO crystals. Radiation damage can be excluded because this effect is uniform within a sub-detector contrary to the radiation fluence, which is however very low at LEP.

Another effect, which we discovered recently, is the calorimeter non-linearity. During the years 1995–1998, LEP gradually increased the beam energy from 45.6 GeV to 94.3 GeV. Every year a calibration run at the Z peak is performed, thus allowing us to disentangle the aging from the non-linearity effect. As it is shown in Figure 8, where the shift is set to zero at 45.6 GeV, the non-linearity is about 0.6% over a range of 50 GeV. We investigated the same effect at low energies using electrons, from radiative Bhabha scattering, with an average energy of 3 GeV. Comparing the ECAL energy measurement with the tracking chamber momentum measurement, we observe an indication of a downward shift of 0.5% compared to the response at 45.6 GeV. However this result is less robust than the one at higher energies for two reasons: the tracking chamber has a limited precision and we must heavily rely on Monte Carlo simulations to estimate the energy loss before the BGO, which is not negligible at low energies.

During the calibration procedure, described in the previous section, aging and non-linearity

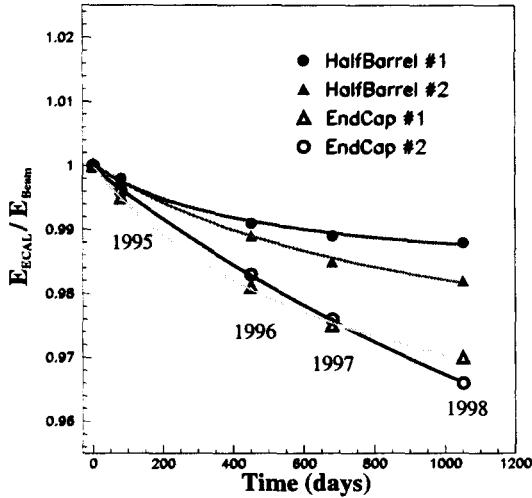


Figure 7. The L3 ECAL aging curves obtained with several LEP runs at a beam energy of 45.6 GeV.

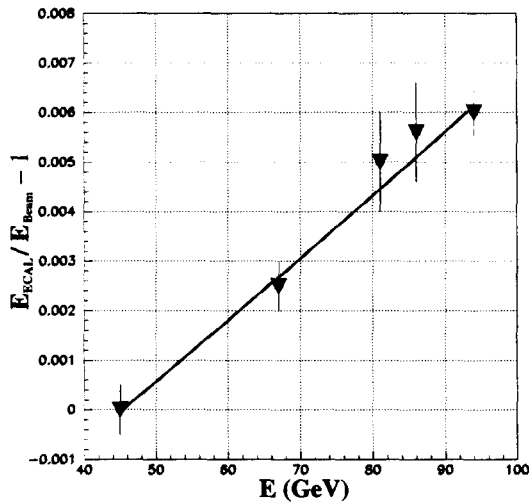


Figure 8. The L3 ECAL non-linearity function obtained with LEP runs at different centre-of-mass energies.

effects are taken into account when combining Bhabha samples collected in different years and at different beam energies.

4. Calibration Accuracy Measurement

An unbiased measurement of the BGO calorimeter energy resolution is performed using a large sample of Bhabha electrons collected in 1998 and not included in the calibration procedure. To fit the Bhabha energy spectrum we

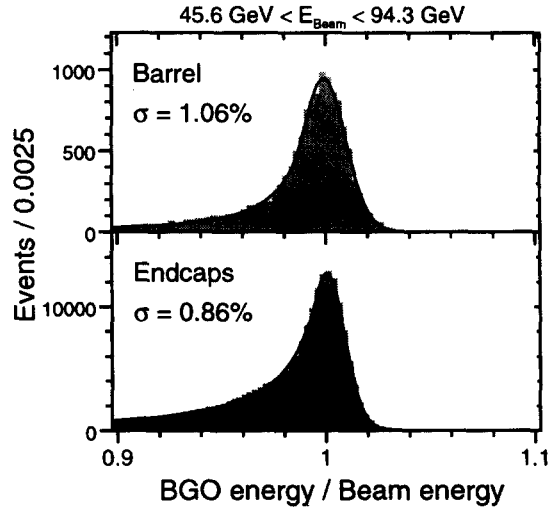


Figure 9. The 1998 Bhabha energy spectra in the barrel and endcaps and superimposed the fit of the function described in the text.

use a function which takes into account resolution effects as well as shower leakages through the support structure where BGO crystals reside. Namely, we fit a Gaussian matched on the low-energy side with a x^{-n} function. The measured ECAL energy resolution is 1.06% in the barrel and 0.86% in the endcaps, as shown in Figure 9. Besides the calibration error, several other factors contribute to the overall energy resolution. Most important are detector related effects such as electromagnetic shower fluctuations, shower leakages, and the accuracy of the temperature determination. Lower energy electrons from residual radiative Bhabha events marginally contribute to the low-energy tail, especially in the endcaps.

The BGO light yield is strongly correlated to the crystal temperature with a coefficient of $-1.55\%/^{\circ}\text{C}$ [2]. Therefore the BGO temperature must be well controlled, especially on the rear face of the crystals where the preamplifiers are mounted. The temperature of every twelfth crystal is continuously monitored by one sensor at the front and one at the back. A two dimensional fit is performed to derive the temperature of all the remaining crystals. The light yield is then corrected according to the estimated temperature at the depth where the maximum of the shower is expected. The uncertainty on this correction reflects in a 0.5% error on the energy measurement.

The intrinsic energy resolution of the L3 BGO

Table 1
L3 ECAL energy resolution for 70 GeV electrons and photons achieved with this calibration.

	Barrel	Endcaps
Intrinsic error	0.8%	0.6%
Temperature error	0.5%	0.5%
Calibration error	0.5%	0.3%
Overall	1.07%	0.84%

detector is limited by electromagnetic shower fluctuations and shower leakages through the carbon fibre support structure where BGO crystals reside. This intrinsic resolution is estimated by means of a detailed simulation of the L3 detector. The resulting errors on the energy measurement, for 70 GeV electrons and photons, are 0.8% and 0.6% in the barrel and in the endcaps, respectively. These errors are different due to the different layout of crystals in the two sub-detectors.

Remaining radiative Bhabha events result in a 0.2% and 0.1% smearing for the endcaps and the barrel energy spectra, respectively. This contribution, estimated by using a Monte Carlo for Bhabha events, is subtracted in quadrature to obtain the true energy resolution of the calorimeter.

From the measured Bhabha energy spectra, shown in Figure 9, and subtracting in quadrature all the known contributions we derive the calibration accuracy, which result in a 0.5% for the barrel and 0.3% for the endcaps. All the relevant contributions to the true energy resolution of the BGO detector are summarised in Table 1. The energy resolution as a function of the electron energy is shown in Figure 10. The energy dependence of the intrinsic error is well described by a function A/\sqrt{E} . The coefficient A is different for the barrel and the endcaps because of the different geometry and amount of material in front of the crystals. The large statistics of the Bhabha sample available for the calibration of the endcaps allows to reduce the calibration error to a negligible level.

5. Conclusion

We presented a new technique for the calibration of a crystal calorimeter based on a RFQ accelerator. We reported results based on the two most successful RFQ runs, taken in 1997 and 1998. These results improve by more than a fac-

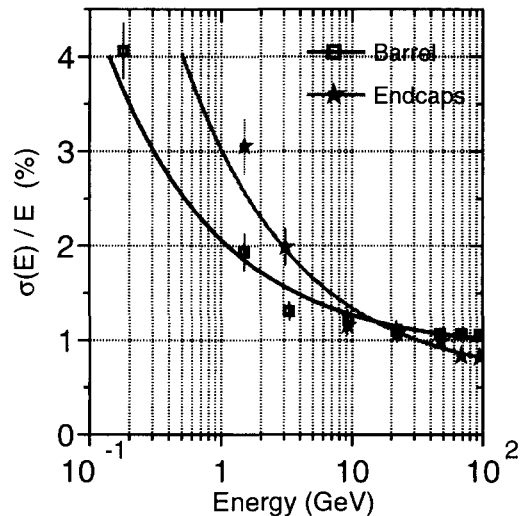


Figure 10. ECAL energy resolution for 1998 data as a function of the electron energy.

tor of two the previous accuracy on the calibration of the BGO detector. This calibration is now in use for the L3 data reconstruction and physics analyses, both for a wide range of new particle searches and for the study of electroweak and QED processes at LEP2.

A calibration precision of 0.5% in the barrel and 0.3% in the endcaps is achieved. This result, which is the best ever obtained since the BGO calorimeter was installed at LEP, is also competitive with the test-beam calibration [2]. The new calibration technique presented in this paper will be used throughout the remainder of the LEP2 physics program, up to centre-of-mass energies of approximately 200 GeV by the year 2000.

REFERENCES

1. L3 Collab., B. Adeva *et al.*, *Nucl. Instrum. Methods A* **289**, 35 (1990).
2. L3 BGO Collab., J. A. Bakken *et al.*, *Nucl. Instrum. Methods A* **280**, 25 (1989) and L3 Note **1712**, (1995).
3. L3 BGO Collab., J. A. Bakken *et al.*, *Nucl. Instrum. Methods A* **343**, 456 (1994).
4. Xenon group, L3 Note **1016**, (1991) and L3 Note **1892**, (1995).
5. R. Y. Zhu *et al.*, *Nucl. Phys. B (Proc. Suppl.)* **44**, 109 (1995).
6. H. Ma *et al.*, *Nucl. Instrum. Methods A* **274**, 113 (1989).